IOP Conf. Series: Materials Science and Engineering **370** (2018) 012034 doi:10.1088/1757-899X/370/1/012034

The Influence of Hoop Diameter on Aerodynamic Performance of O-Ring Paper Plane

N. I. Ismail[1,a], Hazim Sharudin[1], R. J. Talib[1], A. A. Hassan[1] and H. Yusoff

Faculty of Mechanical Engineering, Universiti Teknologi Mara, Kampus Pulau Pinang, 13500 Permatang Pauh, Pulau Pinang, Malaysia.

[a]Corresponding's author: iswadi558@ppinang.uitm.edu.my

Abstract. The O-ring paper plane can be categorized as one of the Micro Air Vehicle (MAV) based on their characteristics and size. However, the aerodynamics performance of the O-ring paper plane was not fully discovered by previous researchers due to its aerodynamics complexity and various hoop diameters. Thus, the objective of this research is to study the influence of hoop diameters towards the aerodynamics performance of O-ring paper plane. In this works, three types of O-ring paper plane known as Design 1, 2 and 3 with different hoop diameter were initially developed by using the ANSYS-Design Modeler. All the design was analyzed based on aerodynamic simulations works executed on ANSYS-CFX solver. The results suggested that Design 3 (with larger hoop size) produced better C_L, C_{Lmax} and AoA_{stall} magnitude compared to other design. In fact, O-ring paper plane with larger hoop size configurations showed potential in providing at least 5.2% and 5.9% better performance in stability ($\Delta C_M/\Delta C_L$) and aerodynamic efficiency (C_L/C_{Dmax}), respectively. Despite the advantages found in lift performances, however, O-ring paper plane with larger hoop size configurations slightly suffered from larger drag increment ($C_{Dincrement}$) compared to smaller hoop size configurations. Based on these results, it can be presumed that O-Ring paper plane with larger hoop sizes contributed into better lift, stability and aerodynamic efficiency performances but slightly suffered from larger drag penalty.

1. Introduction

Micro Air Vehicle (MAV) is defined as a small, portable flying vehicle designed for performing reconnaissance and surveillance missions. MAV also known as a micro scale class of Unmanned Aerial Vehicle (UAV). A basic MAV flight control system includes a miniature receiver with a wire antenna, two miniature servos to drive elevons, an electronic speed controller, and a radio controller with an uplink command transmitter[1]. There are lots of advantages of MAV includes silence, stealth, diminutive and practically undetectable. Due to the MAV characteristics, it has numerous potential applications for both military and civilian[2]. Based on the previous study, MAV can be categorized according to 5 basic types known as flapping, fixed, membrane flexible, rotary and morphing [3]as shown in Figure 1. At maximal dimension of 15 cm and nominal flight speeds of around 10 m/s[4], MAVs can perform missions such as environmental monitoring, surveillance, and assessment in hostile situations. MAV normally operated at Reynolds number range between 10,000 and 100 000, however the flow separation at this Reynolds Number range has led to sudden increases in drag and aerodynamic efficiencies loss.

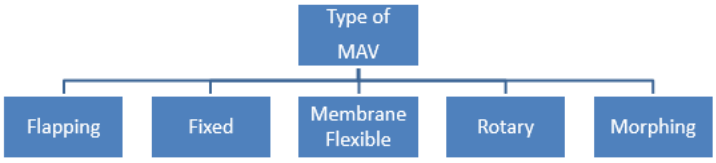

Figure 1. Category of MAV

Through a generation, paper plane has been introduced as an introduction to aeronautical engineering for some many ages. Paper plane is a simple glider that made out from a piece of paper. By using the standard origami technique, the paper plane can be fold into any desired shape and the size of the wingspan also can be adjusted during the folding process[5]. Paper plane can be categorized as one of the MAV because of their sizes. In recent times, paper plane has undergone many changes in terms of their design. O-Ring paper plane (Figure 2) can be categorized as one of the evolution of paper plane designs which is unconventional and complex design. This type of wing is also known as closed wing[6]. Although the O-Ring paper planes are easy to produce, the aerodynamics performances behind this kind of paper plane is still not fully discovered because of its aerodynamics complexity and various hoop sizing. Thus, the objectives of this works to study the influence of hoop diameters towards the aerodynamics performance of O-ring paper plane. In this works, the O-ring CAD designs are initially developed by using the ANSYS-Design Modeler before the aerodynamic analysis was executed based on ANSYS-CFX simulation works. Three types of O-ring paper plane with different hoop sizing known as Design 1, 2 and 3 are used for comparison works.

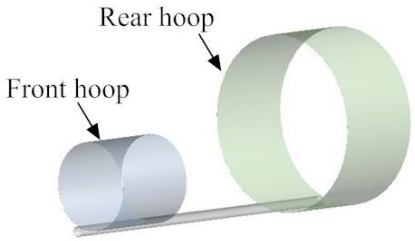

Figure 2. O-Ring paper plane

2. Methodology

In the present research, the O-ring CAD designs are initially developed by using the ANSYS-Design Modeler before the aerodynamic analysis was executed based on ANSYS-CFX simulation works. To solve the turbulent flow issue, 3D RANS equations coupled with SST k-ω turbulent equation are employed under the assumption of a steady, incompressible and turbulent airflow field.

2.1. O-ring paper plane model

The O-Ring paper plane models were develop based on its common configuration in which the front hoop will be smaller than the rear hoop configuration. For comparison works, three selected designs known as is Design 1, Design 2 and Design 3 were used. Each design has different hoop configurations as presented in Table 1 and Figure 3.

2.2. Domain Sizing and Mesh Generation

All the simulation method used in this works were set up in the ANSYS-Workbench framework. The O-Ring CAD design was sliced into half to ease the simulation process and shorten the simulation time. The airflow domain was built surrounding the O-Ring design based on standard sizing as shown in Figure 4. All the O-Ring paper plane part and domain were combined as one-part to ensure that the mesh conforming characteristics achieved in the flow domain. Unstructured hybrid mesh and inflation layers with ANSYS SOLID 187 3D element type was created for all design. The first cell above the

hoop surface is set at $y^+ \leq 1$. Results of the grid independent study shows that the optimized grid achieved around 727745 elements as shown in Figure 5.

Table 1. The characteristic of the 3 selected designs

O-Ring Design	Design 1	Design 2	Design 3
Front hoop diameter	50 mm	70 mm	90 mm
Rear hoop diameter	100 mm	120 mm	140 mm
Wing area	7800 mm^2	9880 mm^2	1190 mm^2
Chord length	52 mm	52 mm	52 mm
Length	200 mm	200 mm	200 mm
Reynold number	100, 139	100, 139	100, 139
Velocity	29.1 m/s	29.1 m/s	29.1 m/s

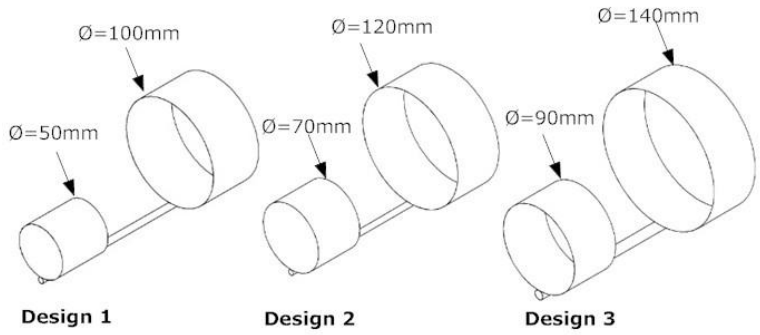

Figure 3. Different hoop sizing on each O-Ring paper plane design

2.3. MAV wing simulation

The boundary conditions imposed on the air domain are also shown in Figure 4. The location of inlet and outlet indicated by flow vectors (Figure 4). The flow velocity was specified at the inlet with velocity of 29.1 m/s. Zero pressure boundary condition is implemented at the outlet to ensure airflow continuities. The symmetrical wall and side walls (opposite the symmetrical wall) imposed as symmetrical and slip surface boundary conditions, respectively. Non-slip boundary surface imposed on hoop surface and automatic wall function is fully employed to solve the flow viscous effect. The angle of attack (AOA) for all O-Ring design was varied between -10° to 40° with 2° interval.

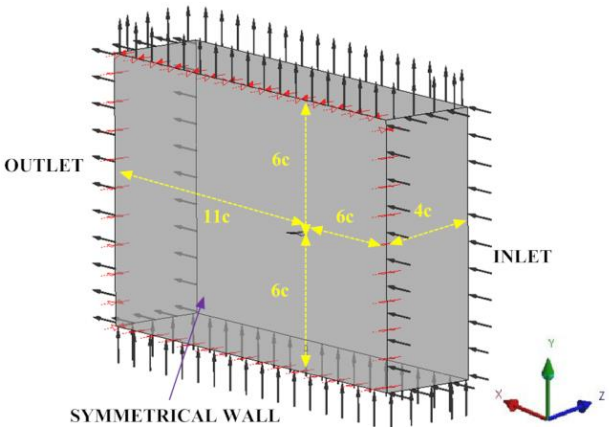

Figure 4. The computational airflow domain sizing and boundary conditions

A steady state, incompressible flow Navier-Stokes equation (RANS) combined with Shear Stress Turbulence (SST) model was used to solve the flow problems over each O-Ring design. The simulation convergence was control based on the magnitude of momentum residual (below 1.0×10^{-5}) and monitoring the stability of of lift coefficient (C_L) and drag coefficient (C_D) value.

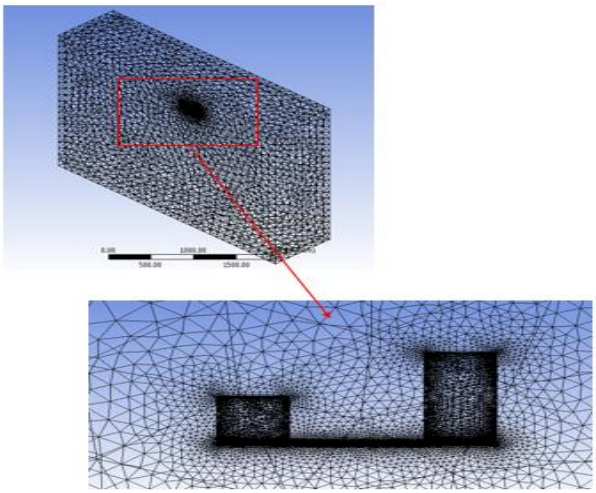

Figure 5. The optimize mesh and inflation layer for ANSYS-CFX solver

3. Results and Discussion

3.1. Aerodynamic performance of O-ring paper plane

Based from the ANSYS-CFX simulation, the aerodynamics performance analysis on each O-Ring design is viewed in detail with particular study given on the aerodynamics performance characteristics such as lift coefficient (C_L), drag coefficient (C_D) and moment coefficient (C_M). The aerodynamic efficiency (C_L/ C_D) was also been analysed based from the of C_L and C_D performances. To show the variation of the aerodynamics performances, each result is presented based on comparison study between the three O-Ring paper plane designs.

3.2. Lift coefficient distribution

Figure 6 shows the C_L performance for all three O-Ring paper plane designs. The graph shows that each design produces a different C_L magnitude but almost similarly in overall trends. In general, the magnitude of C_L for each design have increased proportionally with the angle of attack (AoA) increment particularly in the pre-stall area (AoA area below the stall angle). The C_L magnitude peaks (C_{Lmax}) at its highest magnitude at the stall angle (AoA_{stall}) before it slightly decreases and almost plateau at the post-stall area (AoA>AoAstall).

Based on the C_L analysis taken at AoA =0º to 20 º, the results show that Design 3 produced better C_L magnitude compared to the other designs. In average, Design 3 produce about 16.6% and 23.3% higher C_L magnitude compared to than Design 2 and Design 1, respectively. Based on the C_{Lmax} results, Design 3 exhibited the highest C_{Lmax} at C_{Lmax}=0.613. This C_{Lmax} magnitude is about 6.3% at and 14.2% higher than Design 2 and Design 3 produced, respectively. In AoA_{stall} analysis, the results exhibited that Design 2 and Design 3 produce almost similar AoA_{stall} magnitude at AoA_{stall} =30º. However, Design 1 has induced the earliest stall angle at AoA_{stall} =26º which is 15.4% earlier than Design 2 and Design 3 produced. Based on these results, it obviously shows that Design 3 and Design 2 with larger hoop sizing has promising advantages in producing better C_L magnitude and C_{Lmax}

performance. Thus, one can presume that the O-ring paper plane with larger hoop size which obviously has larger aspect ratio potentially induces the better C_L performances.

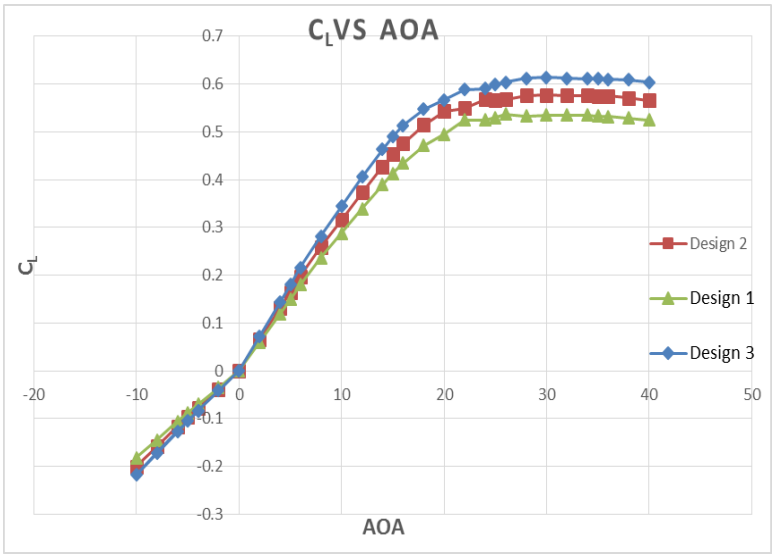

Figure 6. C_L performances for all O-Ring paper plane designs.

3.3. Drag coefficient distribution

The aerodynamic studies of O-Ring paper plane continued on the drag coefficient (C_D) performance as shown in Figure 7. Based on the simulation results, the results exhibited that each designs produced almost consistent and similar C_D trend throughout the AoA range. Generally, the C_D magnitude for each design increase with the AoA increment.

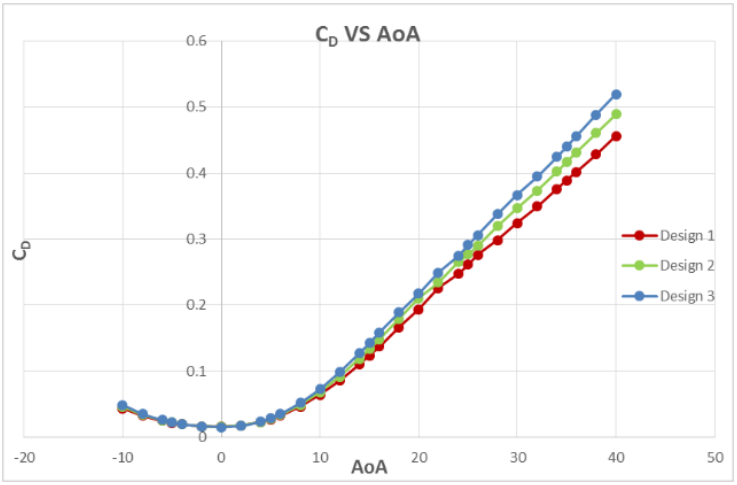

Figure 7. C_D performances for all three O-Ring paper plane design.

Based on the minimum drag magnitude ($C_{D\ min}$) analysis, the results indicated that all three designs exhibited the lowest C_D magnitude at AoA=0º. The detail analysis shows that Design 3 produced the lowest $C_{D\ min}$ among the design at $C_{D\ min}$ =0.01546. Design 2 produced the $C_{D\ min}$ =0.0157 which is 1.4% higher than Design 3 while Design 1 produce the highest $C_{D\ min}$ value of at $C_{D\ min}$ =0.016. This value is about 3.5% higher than the $C_{D\ min}$ magnitude of found in Design 3. Despite the $C_{D\ min}$ advantages, the magnitude of C_D increment ($C_{D\ increment}$) of Design 3 is the highest among the design at

$C_{D\ increment}$ = 22.82% particularly at AoA =0º to 20 º. This is followed by Design 2 and Design 1 at $C_{D\ increment}$ = 22.33% and 21.36%, respectively. However, based on comparative study, the difference in $C_{D\ increment}$ between the designs is below 2%. Thus, one can be presumed that larger hoop size may induced larger drag penalty. This is due to larger surface area found in Design 3 and Design 2 which expose and interact to the airflow which may contribute into the larger skin drag[7].

3.4. Moment coefficient distribution

The graph in the Figure 8 shows the simulation results for the pitching moment coefficient (C_M) performance that has been measured at the wing leading edge. The results indicate that each designs produced almost consistence C_M curve throughout angle of attack range. In general, the magnitude of C_M for all three designs decreased in a non-linear pattern as the value of the C_L increase. The trend clearly shows that the non-linear C_M curve began at the $-C_L$ magnitude up to the C_{Lmax} magnitude before the C_M curve started to induce an irregular pattern. Analysis on C_M results is specifically focused to capture the C_M slope magnitude ($\Delta C_M / \Delta C_L$) which taken at the AoA 5º to 20º. The initial analysis shows that each design produced a negative $\Delta C_M / \Delta C_L$ magnitude which use as an initial indicator for aircraft stability during the flight [8].

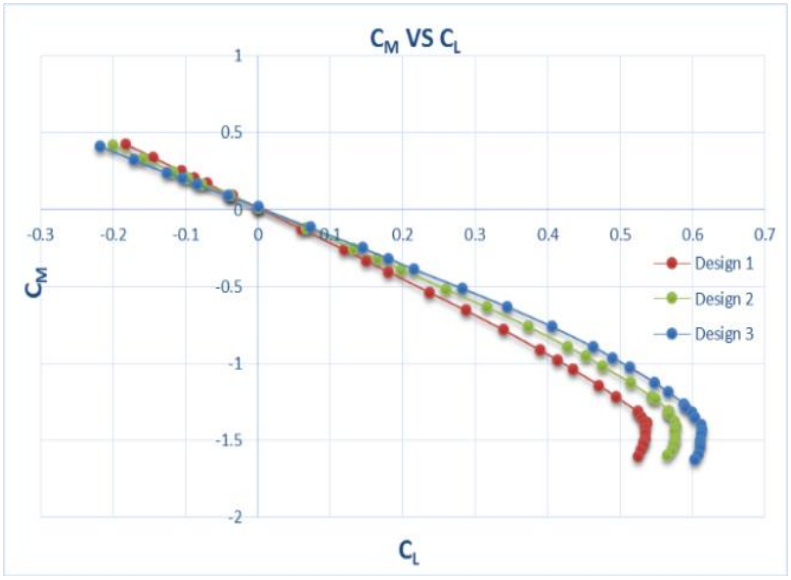

Figure 8. C_M performances on three O-Ring paper plane design.

Based on $\Delta C_M / \Delta C_L$ analysis, Design 3 exhibited the steepest slope magnitude at $\Delta C_M / \Delta C_L$ = -0.444. Design 2 and Design 1 generated lower $\Delta C_M / \Delta C_L$ magnitude at $\Delta C_M / \Delta C_L$ = -0.4222 and -0.396 respectively. This $\Delta C_M / \Delta C_L$ magnitude is about 5.2% (Design 2) and 12.1% (Design 1) lower than Design 3 produced. In aerodynamics study, the $\Delta C_M / \Delta C_L$ magnitude are used to indicate the level of stability for an aircraft. Steeper $\Delta C_M / \Delta C_L$ slope means better stability on MAV wing [8]. Thus, based on this statement, one can presumed that Design 3 is the the most stable among the design. In fact, larger hoop size (found in Design 3 and Design 2) induced better stability O-Ring paper plane.

3.5. Aerodynamic efficiency

The graph in the Figure 9 presents the aerodynamic efficiency (C_L/C_D) for all three design of O-Ring paper plane. In general, the C_L/C_D curves for the all designs increased linearly and peaks approximately at C_L = 0.16 - 0.18. The peak point for the C_L/C_D magnitude is known as the maximum aerodynamic efficiency ($C_L/C_{D\ max}$). Based on the $C_L/C_{D\ max}$ magnitude, the result shows that each

design induced the C_L/C_{Dmax} at the low AoA value between 5º to 6º (or equivalent to $C_L = 0.16 \sim 0.18$). Then, C_L/C_D curve starts to decrease after $C_L/C_{D\,max}$ up to the $C_{L\,max}$ point (AoA_{stall}).

The detail study on $C_L/C_{D\,max}$ magnitude has been conducted to explain the maximum aerodynamic efficiency for all designs. The result shows that Design 3 generated the highest C_L/C_{Dmax} magnitude at 6.27403. This is followed by Design 2 and Design 1 at $C_L/C_{D\,max}$ =5.92613 and $C_L/C_{D\,max}$ =5.5559, respectively. Based on these $CL/C_{D\,max}$ results it shows that Design 3 produce about 5.9% and 13.1% better $C_L/C_{D\,max}$ magnitude than Design 2 and Design 1, respectively. This is possibly due to bigger surface area found in Design 3 which induce better C_L distribution and consequently enhance the C_L/C_{Dmax} performance. From this result, one can presume that the O-Ring with bigger hoop size induces the better $C_L/C_{D\,max}$ performances.

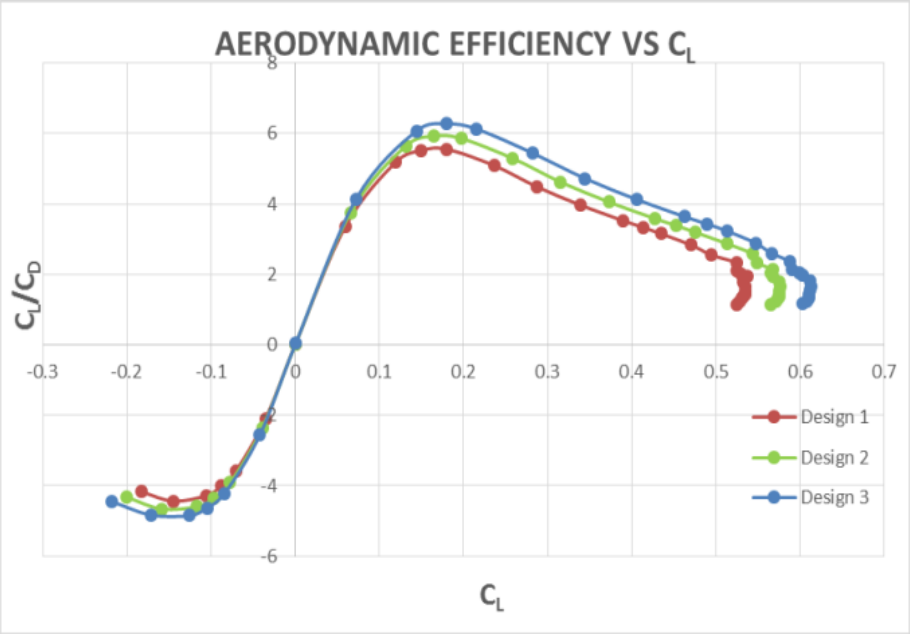

Figure 9. C_L/C_D performances for all thee O-Ring paper plane designs.

4. Conclusion

In this work, the O-Ring paper plane known as Design 1, Design 2 and Design 3 are compared to evaluate the influence of hoop sizing towards the aerodynamic performances. The comparison works have been done by focusing on the common aerodynamic performances such as C_L, C_D, C_M and C_L/C_D.

Based on C_L performance, the result shows that Design 3 produces at least 16.6% higher C_L magnitude compared to other design. In fact, O-Ring paper plane larger hoop configuration (as found in Design 3 and Design 2) produced better C_{Lmax} and AoA_{stall} magnitude compared to smaller hoop configuration.

Based on C_D performance, the result shows that the O-Ring paper plane with larger hoop configuration (Design 3) able to produce at least 1.4% better $C_{D\,min}$ compared to smaller hoop configurations (Design 2 and Design 1). However, Design 3 slightly suffer from larger $C_{D\,increment}$ with at least 2% larger $C_{D\,increment}$ magnitude compared to Design 2 and Design 1.

Based on ΔC_M / ΔC_L analysis, Design 3 promisingly exhibited the steepest slope magnitude at $\Delta C_M/\Delta C_L$ = -0.444 which is about 5.2% and 12.1% better than Design 2 and Design 1 produced, respectively. Steeper ΔC_M / ΔC_L slope means better stability on MAV wing. Thus, the results clearly show that larger hoop size (found in Design 3 and Design 2) induced better stability O-Ring paper plane.

The detail study on C_L/C_{Dmax} magnitude reveals that Design 3 exhibited the highest C_L/C_{Dmax} magnitude at 6.27403. This magnitude is about 5.9% and 13.1% better than Design 2 and Design 1

produced, respectively. This result indicates that larger larger hoop size configuration (found in Design 3 and Design 2) contributes into better the aerodynamic efficiency on O-Ring paper plane.

In conclusions, one can presume that O-Ring paper plane with larger hoop sizes contributes into better lift, stability and aerodynamic efficiency performances. However, it may slightly suffer from larger drag penalty probably due to larger skin drag friction. In future works, an experimental study will be conducted to assess the O-Ring paper plane configurations with view to validate the simulation results.

Acknowledgement

Authors acknowledge technical and financial support from Universiti Teknologi MARA Cawangan Pulau Pinang and the Government of Malaysia.

References

[1] H. Liu, X. Wang, T. Nakata, and K. Yoshida, "Autonomous Control Systems and Vehicles," vol. 65, 2013.

[2] H. Wu, D. Sun, Z. Zhou, S. Xiong, and X. Wang, "Micro Air Vehicle: Architecture and Implementation," in *International Conference 0n Robotics & Automation*, 2003, pp. 1–6.

[3] N. I. Ismail, "Aerodynamic Performances and Flow Structure Investigations On Active Twist Morphing MAV Wing," Universiti Teknologi MARA, 2014.

[4] N. I. Ismail, M. A. Tasin, R. J. Talib, A. H. Zulkifl, M. H. Basri, and M. M. Mahadzir, "A Review on MAV Design Challenges," *Australian Journal of Basic and Applied Sciences*, vol. 10, no. 7, pp. 84–90, 2016.

[5] N. B. Feng, K. Q. Mei, P. Y. Yin, and J. U. Schlüter, "On the Aerodynamics of Paper Airplanes," in *27th AIAA Applied Aerodynamics Conference*, 2009, no. June, pp. 1–16.

[6] P. Roglev, "MDO Framework for Conceptual Design of Closed Wing UAV," *International Journal of Scientific Research Engineering & Technology (IJSRET)*, vol. 2, no. 8, pp. 526–531, 2013.

[7] N. I. Ismail, "Aerodynamic Performances of Twist Morphing MAV Wing," PhD Thesis Dissertation, Universiti Teknologi MARA, 2015.

[8] N. I. Ismail, A. H. Zulkifl, M. Z. Abdullah, M. H. Basri, N. S. Abdullah, A. H. Zulkifli, M. Hisyam Basri, and N. Shah Abdullah, "Computational Aerodynamic Analysis on Perimeter Reinforced (PR)-Compliant Wing," *Chinese Journal of Aeronautics*, vol. 26, no. 5, pp. 1093–1105, Oct. 2013.